

## Sound propagation at frequencies from 3 to 21 MHz in hcp and bcc $^3\text{He}$ and its interaction with dislocations

J. R. Beamish\* and J. P. Franck

*Department of Physics, University of Alberta, Edmonton, Alberta T6G 2J1, Canada*

(Received 24 May 1982; revised manuscript received 7 September 1982)

The velocity and attenuation of longitudinal sound were measured at various molar volumes in both bcc and hcp  $^3\text{He}$  and, for comparison, in hcp  $^4\text{He}$ . The measurements were made between 80 mK and melting at frequencies between 3 and 21 MHz. Below about one-half of the melting temperature, the sound velocity deviated from the adiabatic form, and the deviation was accompanied by large increases in the attenuation. This anomalous behavior, observed in both bcc and hcp  $^3\text{He}$  crystals, as well as in hcp  $^4\text{He}$ , could be qualitatively explained by the Granato-Lücke theory of dislocation-sound-wave interactions. From the temperature and frequency dependence of the velocity anomaly, the dislocation density  $\Lambda$ , average pinning length  $L$ , and damping constant  $B$  were determined. Typical values were  $\Lambda = 10^5 \text{ cm}^{-2}$ ,  $L = 10^{-3} \text{ cm}$ , and  $B = 2 \times 10^{-7} T^3$  cgs units when an exponential distribution of loop lengths was assumed. The attenuation agreed at least qualitatively with the predictions of the Granato-Lücke theory. At low densities in bcc  $^3\text{He}$ , the anomaly was absent.

### I. INTRODUCTION

Because of the large zero-point motion of its atoms, solid helium is referred to as a quantum solid. Its quantum properties are most clearly reflected in the behavior of lattice defects. Vacancies and isotopic impurities in solid helium have been studied by NMR techniques<sup>1</sup> which fairly directly demonstrate their quantum properties. Dislocations, however, have only been studied by indirect methods. Ultrasonic measurements of the sound velocity and attenuation have proven very useful in the study of dislocation properties in solid helium.

In hcp  $^4\text{He}$ , the existence of dislocations has been inferred from the mosaic spread observed in neutron-diffraction measurements,<sup>2</sup> from the mobility of ions,<sup>3</sup> and from plastic flow experiments.<sup>4</sup> Ultrasonic measurements in hcp  $^4\text{He}$  (Refs. 5–7) have shown an anomalous behavior which has also been attributed to dislocations. The anomaly consisted of frequency-dependent deviations of the sound velocity from the expected adiabatic temperature dependence. These deviations, which occurred below about one-half of the melting temperature and varied in size and shape from sample to sample, were accompanied by large increases in the sound attenuation. The velocity anomaly was first interpreted in terms of dislocations by Wanner *et al.*,<sup>5</sup> who obtained good agreement with their data at a single frequency (8 or 12 MHz) by using the Granato-Lücke theory<sup>8</sup> of dislocation-sound-wave

interactions and assuming two effective dislocation loop lengths. Iwasa *et al.*<sup>7</sup> used a continuous exponential distribution of loop lengths to fit their velocity data at frequencies of 10, 30, and 50 MHz. In addition, they obtained qualitative agreement with their attenuation measurements. Measurements of the shear modulus and internal friction at 331 Hz (Ref. 9) and at 15 kHz (Ref. 10) were also in agreement with the Granato-Lücke model of vibrating dislocations.

In contrast to the situation in hcp  $^4\text{He}$ , ultrasonic measurements in bcc  $^3\text{He}$  (Refs. 11 and 12) showed neither a velocity nor an attenuation anomaly. There are several possible reasons for this difference. The two most obvious are the differences in isotope (Fermi versus Bose statistics) and in crystallographic phase (bcc versus hcp). In addition, the hcp  $^4\text{He}$  measurements were made at densities between 17 and 20  $\text{cm}^3/\text{mole}$ , while the bcc  $^3\text{He}$  measurements were at much lower densities (around 24  $\text{cm}^3/\text{mole}$ ). Finally, it was observed<sup>5,13</sup> that adding about 100 ppm of  $^3\text{He}$  to the hcp  $^4\text{He}$  suppressed the anomaly and the bcc  $^3\text{He}$  samples contained significant amounts of  $^4\text{He}$ .

We report here the first measurements of the sound velocity and attenuation of high-purity  $^3\text{He}$  crystals (1.35 ppm  $^4\text{He}$ ) at various densities in both the bcc and the hcp phases. The results are analyzed in terms of the Granato-Lücke theory. For comparison, measurements were also made on hcp  $^4\text{He}$  and analyzed in the same manner. Prelimi-

nary results of the experiments have been reported elsewhere.<sup>14</sup>

## II. EXPERIMENTAL METHOD

The crystals studied were grown at constant pressure (between 35 and 185 bar) from <sup>3</sup>He which was later analyzed<sup>15</sup> as containing 1.35 ppm of <sup>4</sup>He. Once the crystal growth was completed, the capillary was blocked and the sound velocity and attenuation were measured as the crystal was cooled at constant volume.

The sample cell is shown in Fig. 1. The cell body was made from hardened beryllium copper and the seals between the various pieces were made either with indium or aluminum *O* rings. The two matched *X*-cut quartz transducers had a fundamental frequency of 3 MHz and could be excited at their harmonics to give 9-, 15-, and 21-MHz signals. They were backed by spring-loaded pistons in order to be self-aligning against a central spacer that had polished parallel sides. The transducer spacing was measured as 0.933 cm using the known sound velocity in liquid <sup>4</sup>He.<sup>16</sup> The total volume of

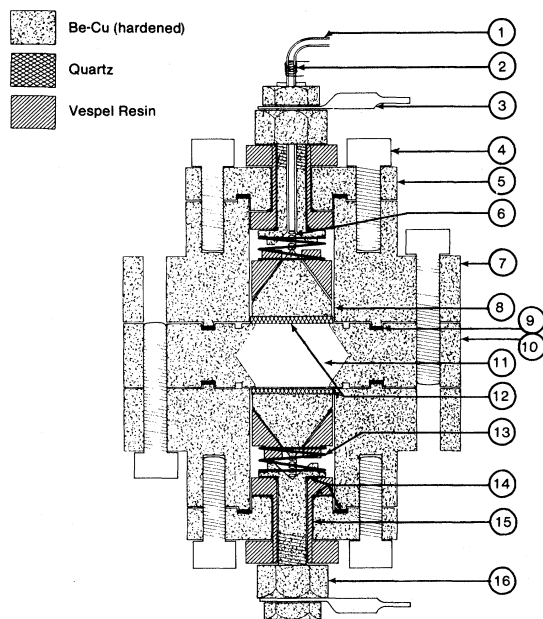


FIG. 1. Sample cell. 1, helium pressure line; 2, pressure line heater; 3, electrical feedthrough; 4, assembling screws; 5, end cap; 6, electric spring-type connector; 7, cell body; 8, transducer backing piston; 9, aluminum gasket; 10, polished parallel transducer spacer; 11, helium space; 12, transducers; 13, transducer retaining spring; 14, indium pressure seals; 15, electrical feedthrough insulation; 16, clamping nut.

the sample space was 2.1 cm<sup>3</sup>. The sample gas was admitted to the cell through 3 m of 0.1-mm-i.d. stainless-steel capillary which was connected by an electrically insulating fitting to a  $\frac{1}{16}$ -in. tube which in turn was soldered into one of the electrical feedthroughs.

The opposite end of the cell was connected by strips of copper foil to the mixing chamber of a SHE minifridge. With the heat load from the capillary, electrical leads, and ultrasonic signal, temperatures of about 80 mK were attained and the cell could be maintained below 200 mK indefinitely. The primary thermometer was a commercially calibrated germanium resistance thermometer (Lakeshore Cryogenics GR-200A-30) which permitted temperatures to be measured to an accuracy of about  $\pm 5$  mK.

The desired <sup>3</sup>He pressure was generated by condensing the <sup>3</sup>He (0.56 moles) into a volume of 24.1 cm<sup>3</sup> which was immersed in liquid <sup>4</sup>He. By pumping on the <sup>4</sup>He, the temperature of the condenser could be reduced to 1.6 K and most of the <sup>3</sup>He condensed. By warming the condenser, pressures up to 200 bar were generated. A similar method was used for the <sup>4</sup>He crystals. The growth pressure was measured using a Heise bourdon tube gauge (0–200 bar,  $\pm 0.1\%$ ) whose internal volume of 13 cm<sup>3</sup> served as a ballast during crystal growth.

Before growing crystals, the cell was flushed with hydrogen gas and thoroughly pumped at room temperature. The cell was then cooled to 4 K and sample gas admitted up to the desired growth pressure. The pressure line heaters were turned on to prevent blockage and the cell was cooled by circulating gas through the minifridge. When freezing began, the pressure was manually maintained within about 0.2 bar by admitting small amounts of gas from the condenser. By this method, crystals were grown at nearly constant pressures with growth rates ranging from about 0.5 to 2 cm/h. Upon completion of crystal growth, as many as 100 ultrasonic echoes were visible, indicating attenuation values as low as 0.3 dB/cm. This low attenuation and the absence of spurious echoes, combined with an observed variation of sound velocities at a single density of about 15%, indicated that the samples were either single crystals or had only low-angle grain boundaries. About 50% of the crystals grown were rejected due to either weak ultrasonic signals or echo envelopes indicating a serious transducer misalignment.

A block diagram of the system used to measure the sound velocity  $v$  and attenuation  $\alpha$  is shown in Fig. 2. The velocity was measured using a modulated-pulse-superposition method similar to

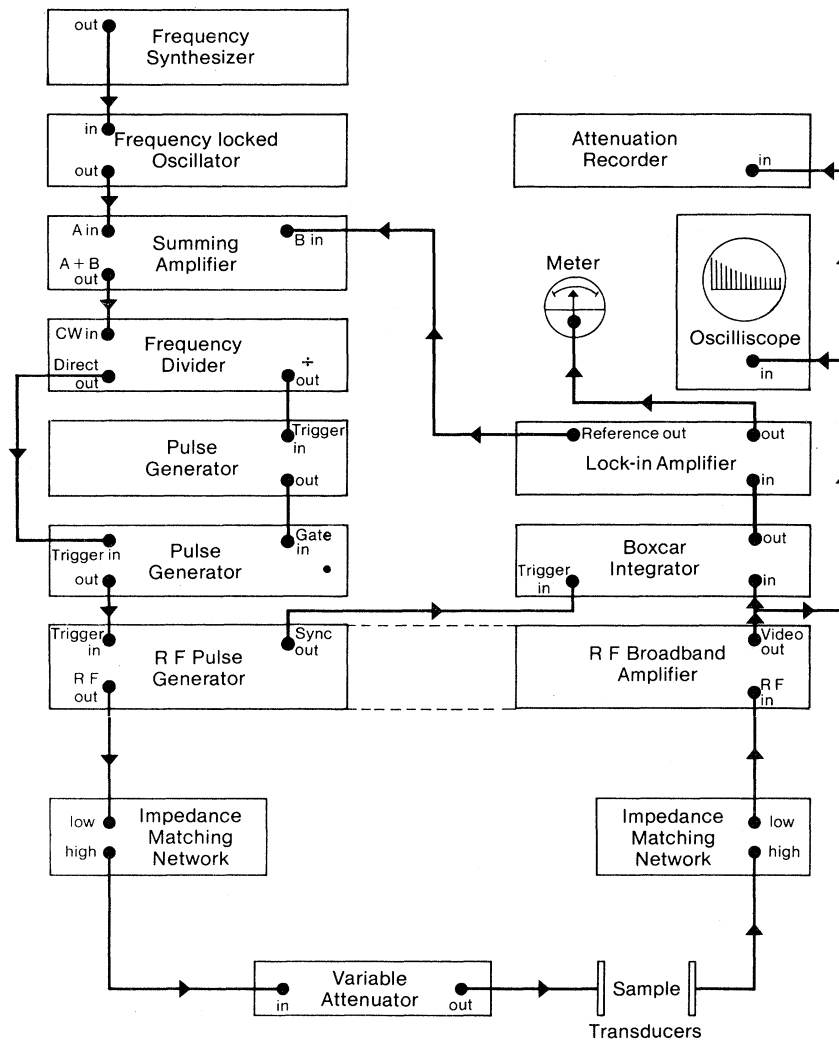


FIG. 2. Block diagram of ultrasonic electronics.

that described by Holder.<sup>17</sup> Several rf pulses separated by approximately one round-trip time were applied to the sending transducer. The frequency synthesizer, which triggered the rf pulse generator, was manually adjusted to maximize the amplitude of the first received echo, indicating an exact rf superposition. The synthesizer frequency was then proportional to the sound velocity. Addition of a boxcar integrator and a lock-in amplifier considerably increased the sensitivity of the system. A velocity resolution of 1 part in  $10^5$  was typically achieved with a stability of about 3 parts in  $10^5$  during one day. The absolute accuracy of the velocity measurements was limited to about  $\pm 0.5\%$  by the uncertainty in the transducer spacing.

Changes in the attenuation were measured by comparing the heights of two selected echoes using a Matec 2470A automatic attenuation recorder.

The sensitivity ranged from 0.02 dB/cm with low attenuation to 0.1 dB/cm when the attenuation was high. The nonexponential echo envelope indicated that the transducers were not perfectly aligned and prevented absolute attenuation values from being measured. At 3 MHz, however, 20 or more echoes were generally visible before the first minimum in the envelope, so this did not seriously affect the relative attenuation measurements. When  $\alpha$  became greater than about 5 dB/cm, the attenuation uncertainties became very large and, for significantly higher attenuations, it was not possible to measure the sound velocity.

During measurements, the pulse repetition rate varied between 200 and 2000 pulses per sec. The stress amplitude in the measuring pulses was estimated as about  $10^3$  dyn/cm<sup>2</sup> at 3 MHz and smaller than 200 dyn/cm<sup>2</sup> at 9 and 21 MHz.

In contrast to some observations in hcp  $^4\text{He}$ ,<sup>18</sup> neither annealing the crystals near melting nor rapidly changing the temperature (at rates up to about 18 mK/sec) affected the ultrasonic signal. During measurements, the crystals were kept at least 100 mK below melting.

### III. METHOD OF ANALYSIS

The experimental results were analyzed by means of the Granato-Lücke theory in a manner similar to that used by Iwasa *et al.*<sup>7</sup> for hcp  $^4\text{He}$ . At high temperatures, in the adiabatic range, the phonon part of the sound-velocity change can be written as<sup>11</sup>

$$\Delta v_a(T) = v_a(T) - v_0 = aT^4 + bT^6. \quad (1)$$

The total velocity change  $\Delta v$  can be written as

$$\Delta v(T) = \Delta v_a(T) + \Delta v_d(T), \quad (2)$$

where  $\Delta v_d$  is the dislocation contribution which can be compared to the Granato-Lücke expression for the dislocation part

$$\frac{\Delta v_d}{v_0} = R \int \frac{\Delta \tilde{v}(l)}{v_0} l N(l) dl, \quad (3)$$

where  $R$  is an orientation factor discussed later.  $N(l) dl$  is the number per unit volume of dislocation loops with lengths between  $l$  and  $l+dl$ . In the analysis to follow, an exponential distribution is assumed:

$$N(l) = \frac{\Lambda}{L^2} \exp\left[-\frac{l}{L}\right], \quad (4)$$

where  $L$  is the average loop length and  $\Lambda$  is the dislocation density. The term  $\Delta \tilde{v}(l)/v_0$  is the contribution to the velocity of a unit density of loops of length  $l$  and is given by

$$\frac{\Delta \tilde{v}(l)}{v_0} = \frac{-4v_0^2}{\pi^3} \frac{\omega^2(l) - \Omega^2}{[\omega^2(l) - \Omega^2]^2 + (B\Omega/A)^2}, \quad (5)$$

where  $\Omega$  is the sound frequency,  $B$  is the dislocation damping,  $A$  is the dislocation effective mass, and  $\omega(l)$  is the resonant frequency of a loop of length  $l$  given by

$$\omega(l) = \left[ \frac{2}{1-\nu} \right]^{1/2} v_t/l. \quad (6)$$

Here,  $\nu$  is Poisson's ratio and  $v_t$  is the transverse

sound velocity.

The corresponding expression for the dislocation contribution to the attenuation is given in the Granato-Lücke theory by

$$\alpha_d = R \int \tilde{\alpha}(l) l N(l) dl, \quad (7)$$

where

$$\tilde{\alpha}(l) = \frac{4v_0}{\pi^3} \frac{\Omega^2 B/A}{[\omega^2(l) - \Omega^2]^2 + (B\Omega/A)^2}. \quad (8)$$

There is a critical value of  $l$ , denoted by  $l_c$ , for which  $\Delta \tilde{v}(l)/v_0$  is zero and  $\tilde{\alpha}(l)$  is maximum. This is given by

$$l_c = \left[ \frac{2}{1-\nu} \right]^{1/2} v_t/\Omega. \quad (9)$$

Loops shorter than  $l_c$  reduce the velocity, while loops longer than  $l_c$  increase it. The sign and shape of the dislocation contribution to  $v$  are determined by the value of the parameter

$$t = \frac{L}{l_c} = \left[ \frac{1-\nu}{2} \right]^{1/2} \frac{1}{v_t} \Omega L. \quad (10)$$

The effective mass  $A$  comes from the elastic energy of the dislocations and is given by  $A = \pi \rho b^2$ , where  $b$  is the Burgers vector. The damping  $B$  comes from interactions between moving dislocations and thermal phonons in the crystal. The phonon-dislocation interaction caused by lattice anharmonicity<sup>19</sup> predicts a damping  $B \propto T^5$  at low temperatures while the fluttering mechanism<sup>20</sup> predicts  $B \propto T^3$ .

The comparison between the experimental data and the Granato-Lücke theory was made as follows. First, the velocity data above about one-half of the melting temperature were fit by a least-squares method to a polynomial of the form  $aT^4 + bT^6$ . Since the dislocation contribution to  $v$  is small at high temperatures, this represented the adiabatic part of the velocity. By subtracting the adiabatic part from  $v$ , the remainder could be interpreted as the dislocation part and could be compared to the dislocation-theory predictions.

From the magnitude of the dislocation contribution to the velocity, the dislocation density  $R\Lambda$  could be determined. From the frequency dependence, the average loop length  $L$  was found. The damping was assumed to be of the form

$$B = gT^n \quad (11)$$

and the exponent  $n$  was determined from the maximum slope of the velocity change  $dv_d/dt$  while the

coefficient  $g$  was found from the temperature at which the maximum slope occurred. The parameters  $RA, L, g, n$  were then varied to get the best overall fit to the velocity data. Since it was not possible to accurately fit the data at all frequencies simultaneously, the emphasis in most cases was on matching the temperature dependence of the 9-MHz data, which usually had the clearest velocity anomaly.

With the use of the dislocation parameters derived from fitting the velocity data, the dislocation attenuation was computed and compared to the measured attenuation. Owing to the limited absolute accuracy of the attenuation measurements, only qualitative comparisons were made.

Note that the fitting procedure did not give the dislocation density  $\Lambda$  directly but rather the combination  $RA$ . If the elastic constants and the operative slip systems are known, the orientation factor  $R$  may be calculated<sup>21</sup> for a given sound-propagation direction and polarization. For hcp  $^4\text{He}$  there is evidence that the slip plane is the basal plane.<sup>18</sup> In hexagonal crystals,  $R$  depends only on the angle  $\theta$  between the normal to the wave front and the  $c$  axis. Although the elastic constants of hcp  $^3\text{He}$  are not known, the orientation factor will be zero for  $0^\circ$  and  $90^\circ$  and will have a maximum value of about 0.1 to 0.2 at an angle of about  $50^\circ$ .

In cubic crystals,  $R$  depends on two crystallographic angles and is much less anisotropic,<sup>22</sup> generally being nonzero at all orientations and varying only between about 0.04 and 0.1.

#### IV. RESULTS AND ANALYSIS

##### A. hcp $^3\text{He}$

Figure 3 shows the relative sound velocity measured at 3, 9, and 21 MHz in an hcp  $^3\text{He}$  crystal grown at a pressure of 145 bar ( $V=18.6 \text{ cm}^3/\text{mole}$ ). The solid lines in Fig. 3 are the results of fitting the velocity data above 1.5 K to polynomials of the adiabatic form  $aT^4 + bT^6$ , Eq. (1). Above about 1 K the fits are good, indicating that the velocity changes were essentially adiabatic. Below 1 K, however, the velocities deviated from the adiabatic curves. The deviations were accompanied by increases in the attenuation. These features are similar to those previously observed in hcp  $^4\text{He}$  and together are referred to as the anomaly.

Both the sound velocity and attenuation were reproducible when the temperature was cycled. The

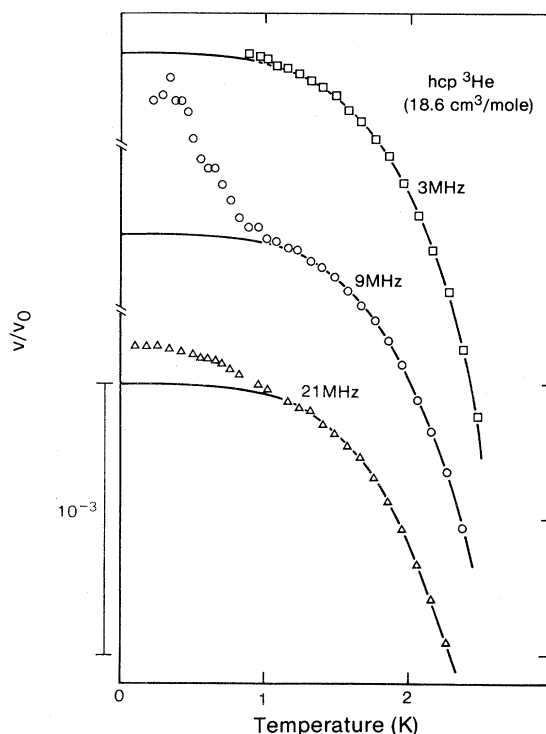


FIG. 3. Sound velocity of an hcp  $^3\text{He}$  crystal at  $18.6 \text{ cm}^3/\text{mole}$  as function of temperature, at three measuring frequencies.

only exception occurred when large-amplitude 3-MHz pulses were applied at temperatures below about 300 mK. In this case, the large pulses reduced the attenuation and changed the sound velocity. When warmed above about one-half the melting temperature, the crystal recovered to its original state, resulting in a reproducible hysteresis upon thermal cycling. This effect, which was observed in both bcc and hcp  $^3\text{He}$  as well as in hcp  $^4\text{He}$ , is believed to be due to partial pinning of dislocations by large stresses. The effect of large pulses has been discussed in a previous paper<sup>14</sup> and will be more fully treated in a subsequent paper. No such effect was observed when 9- or 21-MHz pulses were applied, and the low-temperature changes in  $v$  and  $\alpha$  could be avoided either by keeping the sample above 300 mK or by keeping the 3-MHz stress amplitude low. In the rest of this paper, the only data discussed will be those taken during cooling, before high-amplitude 3-MHz pulses were applied.

Below 1 K, the 3-MHz attenuation became so large that velocity measurements were impossible, and so no 3-MHz velocity anomaly could be observed at low temperatures. However, the positive

velocity anomaly at 9 MHz and the smaller but still positive one at 21 MHz are suggestive of a dislocation contribution to  $v$ . Because of this similarity and the success of previous dislocation explanations of hcp  $^4\text{He}$  anomalies, the measured velocity and attenuation were compared to the Granato-Lücke theory of dislocations.

Since the anomaly observed during cooling was reproducible, depending neither on the cooling rate nor on any annealing of the crystal, it was assumed that the dislocation density and loop length distributions did not change. To make quantitative comparisons between theory and the experimental data, the exponential distribution of Eq. (4) was chosen and the dislocation damping was assumed to be of the form  $B = gT^n$ . The four dislocation parameters ( $R\Lambda, L, g, n$ ) were then determined by fitting the velocity anomaly to computed curves for the dislocation contributions to  $v$ .

Figure 4(a) shows the results of such a fit to the velocity data from the hcp  $^3\text{He}$  crystal shown in Fig. 3. The adiabatic part of the temperature dependence has been subtracted out, leaving only the anomalous part of the velocity. The solid curves in Fig. 4(a) are the dislocation contributions calculated for the choice of dislocation density  $R\Lambda = 1.84 \times 10^3 \text{ cm}^{-2}$ , average loop length  $L = 6.37 \times 10^{-3} \text{ cm}$ , and damping  $B = 1.41 \times 10^{-7} T^3 \text{ cgs units}$ . Although the 9-MHz fit is good, the predicted anomaly at 21 MHz is somewhat smaller than that actually observed. The 3-MHz measurements do not extend to sufficiently low temperature to allow meaningful comparison to the Granato-Lücke predictions.

Figure 4(b) shows the measured changes in attenuation corresponding to the velocity data of Fig. 4(a). The rise in  $\alpha$  at low temperatures is typical of vibrating dislocation lines. The solid curves shown in Fig. 4(b) are the predictions of the Granato-Lücke theory using the dislocation parameters from the velocity fit of Fig. 4(a). Although the measured changes in  $\alpha$  are several times smaller than predicted, they agree qualitatively with the Granato-Lücke values. The relative sizes of the 3-, 9-, and 21-MHz attenuation are correctly predicted and maxima were observed in the 9- and 21-MHz attenuation at approximately the same temperatures as the maxima in the theoretical curves.

The quoted dislocation parameters are somewhat uncertain. The choice of  $n = 3$  for the damping-temperature exponent gave considerably better agreement with the experimental temperature dependence of  $v$  than either  $n = 2$  or 5 but only

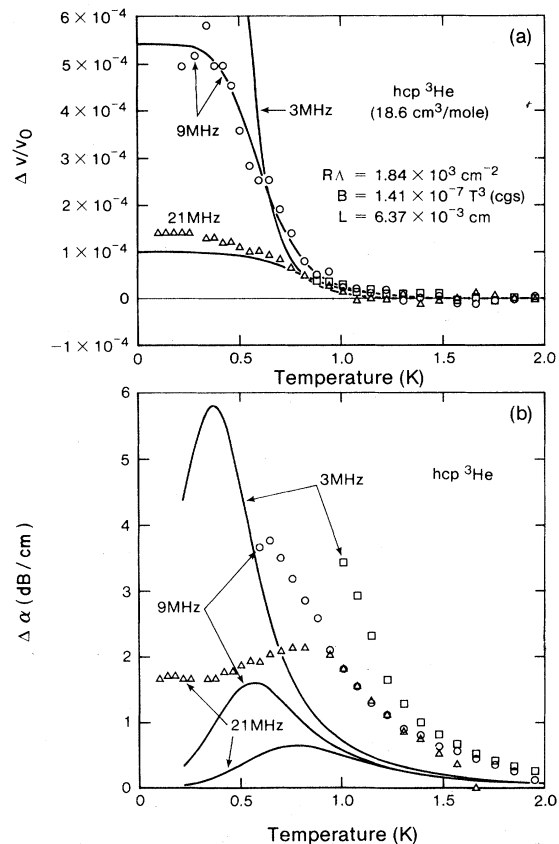


FIG. 4. Measured dislocation contribution to sound velocity and attenuation for the same hcp  $^3\text{He}$  crystal as shown in Fig. 3. Solid lines represent a fit to Granato-Lücke theory using the parameters indicated.

slightly better than  $n = 4$ . Since it was not possible to simultaneously fit the 9- and 21-MHz data, the dislocation parameters given are those for a fit to the 9-MHz data. A fit of the 21-MHz velocity gave  $RA = 2.63 \times 10^3 \text{ cm}^{-2}$ ,  $L = 6.37 \times 10^{-3} \text{ cm}$ , and  $B = 1.71 \times 10^{-7} T^3 \text{ cgs units}$ . The value of  $L$  is rather uncertain since the relative sizes of the 9- and 21-MHz anomalies were insensitive to the value of  $L$ . It should be remembered that the dislocation parameters determined in this way are valid only for an exponential distribution of loop lengths.

Several other hcp  $^3\text{He}$  crystals were grown at the same density ( $18.6 \text{ cm}^3/\text{mole}$ ). The anomaly and dislocation fit for one other crystal are shown in Fig. 5. The velocity fit is good and the attenuation predicted using the resulting dislocation parameters agrees quite well with the measured attenuation. The anomaly in this crystal was an order of magnitude smaller than in the previously discussed crystal. The dislocation parameters found from the fit were  $RA = 1.70 \times 10^2 \text{ cm}^{-2}$ ,  $L = 1.02 \times 10^{-3} \text{ cm}$ ,

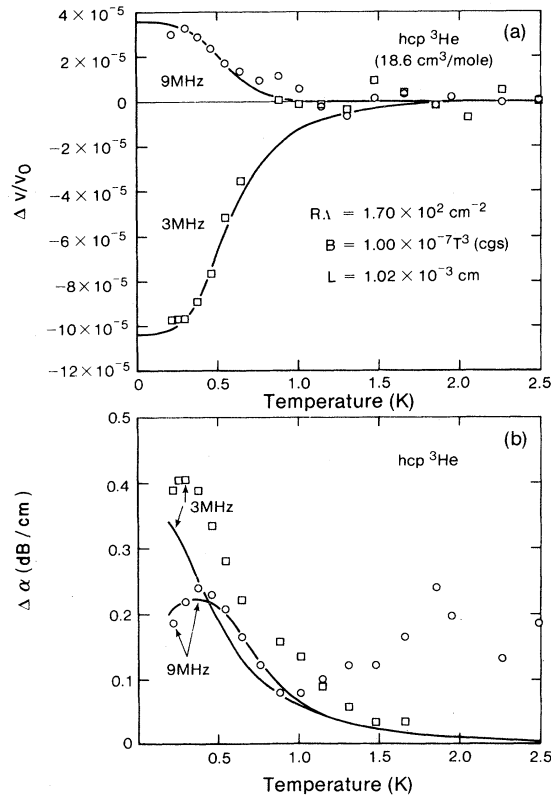


FIG. 5. Measured dislocation contribution to sound velocity and attenuation for a different hcp  $^3\text{He}$  crystal at  $18.6 \text{ cm}^3/\text{mole}$ . Solid lines represent fit to Granato-Lücke theory using the parameters shown.

and  $B = 1.00 \times 10^{-7} T^3$  cgs units. The average loop length in this crystal was rather small, resulting in a negative 3-MHz velocity anomaly. The damping  $B$ , however, had the same temperature dependence ( $B \sim T^3$ ) and roughly the same magnitude in both crystals, a reasonable result since the damping depends only on dislocation-phonon interactions and so should be independent of the dislocation densities and loop lengths.

The other crystals grown at this density had similar anomalies. A few hcp  $^3\text{He}$  crystals were grown at higher pressure at 185 bar ( $V = 17.8 \text{ cm}^3/\text{mole}$ ). These too showed an anomaly similar to the  $18.6 \text{ cm}^3/\text{mole}$  crystals. The dislocation parameters for the only crystal at  $V = 17.8 \text{ cm}^3/\text{mole}$  with sufficient data for a fit to be made were  $RA = 4.32 \times 10^3 \text{ cm}^{-2}$ ,  $L = 7.30 \times 10^{-4} \text{ cm}$ , and  $B = 5.73 \times 10^{-8} T^3$  cgs units.

#### B. bcc $^3\text{He}$

Measurements were made on bcc  $^3\text{He}$  at three densities (20.1, 22.3, and  $24.2 \text{ cm}^3/\text{mole}$ ). The 20.1

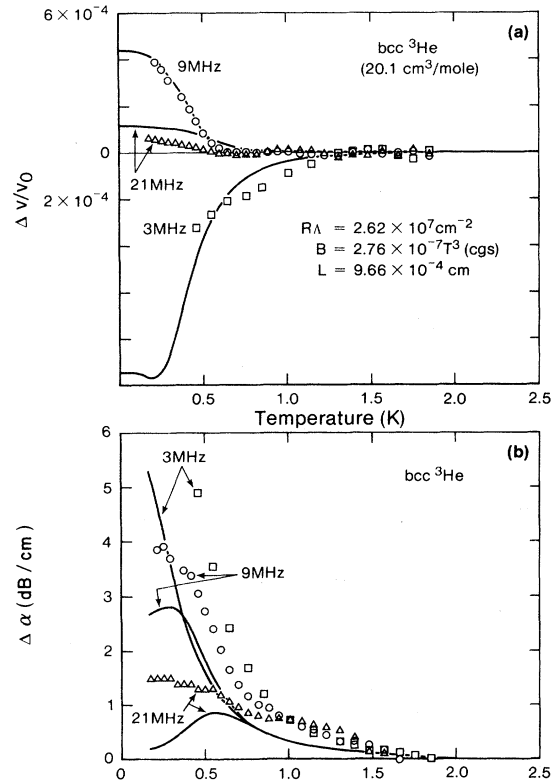


FIG. 6. Measured dislocation contribution to sound velocity and attenuation for a bcc  $^3\text{He}$  crystal at  $20.1 \text{ cm}^3/\text{mole}$ . Solid lines represent fit to Granato-Lücke theory using the parameters shown.

$\text{cm}^3/\text{mole}$  crystals (growth pressure of 100 bar) had anomalies similar to those in hcp  $^3\text{He}$ . Figure 6 shows the anomaly in one bcc crystal. The dislocation density  $RA = 2.62 \times 10^3 \text{ cm}^{-2}$  and average loop length  $L = 9.66 \times 10^{-4} \text{ cm}$  are about the same magnitude as in hcp  $^3\text{He}$  but the damping  $B = 2.76 \times 10^{-7} T^3$  cgs units is about twice as large. The other bcc  $^3\text{He}$  crystals grown at this density had very similar anomalies.

Crystals of bcc  $^3\text{He}$  were also grown at 22.3 and  $24.2 \text{ cm}^3/\text{mole}$ . The  $22.3 \text{ cm}^3/\text{mole}$  crystals had an anomaly which was about one-fifth as large as at  $20.1 \text{ cm}^3/\text{mole}$  but was otherwise similar. The smallness of the anomaly prevented dislocation parameters from being determined.

Figure 7 shows the velocity and attenuation in a crystal of molar volume  $24.2 \text{ cm}^3/\text{mole}$ . Within the experimental resolution there was no velocity anomaly and the attenuation decreased below 0.4 K. This absence of an anomaly agrees with the results of previous measurements at this density.<sup>11,12</sup> The absence of an anomaly in those earlier measurements was therefore probably due to the low densi-

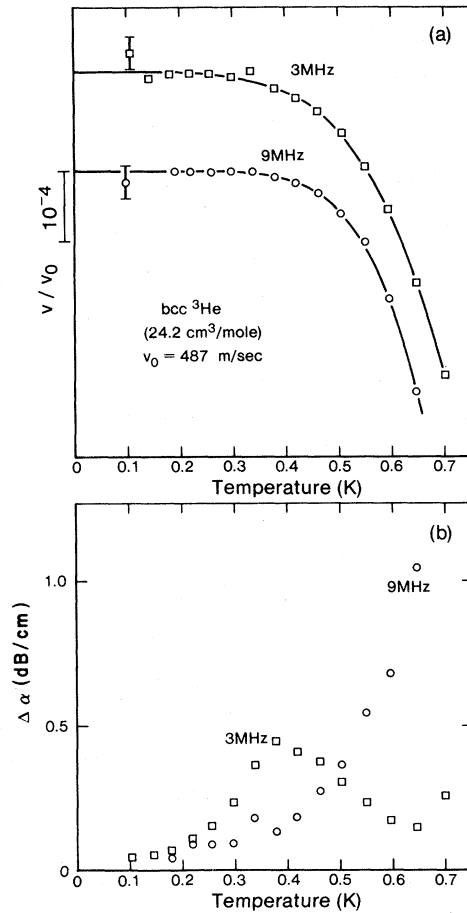


FIG. 7. Sound velocity and attenuation for a bcc  $^3\text{He}$  crystal at  $24.6$  cm<sup>3</sup>/mole, at two measuring frequencies, 3 and 9 MHz. Solid lines are fit to adiabatic variation of sound velocity.

ty, rather than to the presence of isotopic impurities.

### C. hcp $^4\text{He}$

As a check on the  $^3\text{He}$  results and in order to allow comparisons to previous work, crystals of hcp

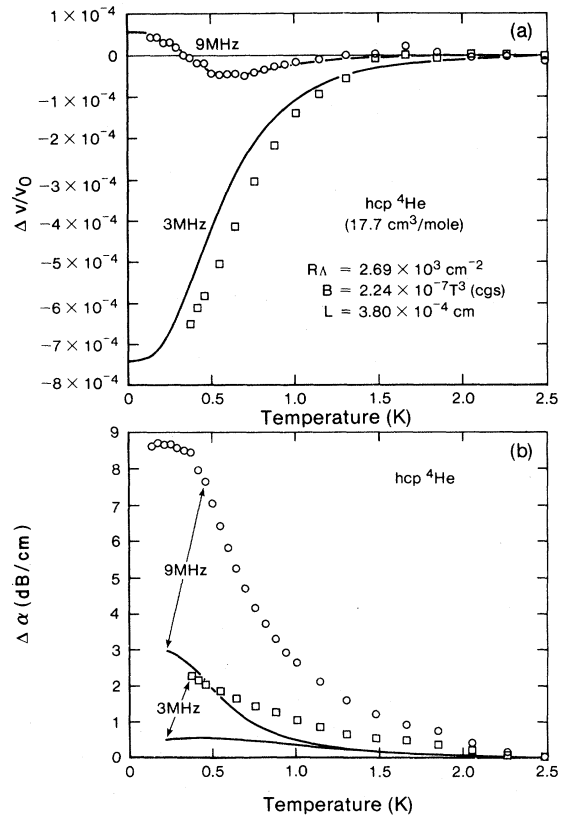


FIG. 8. Measured dislocation contribution to sound velocity and attenuation for a hcp  $^4\text{He}$  crystal at  $17.7$  cm<sup>3</sup>/mole. Solid lines are fit to Granato-Lücke theory using parameters shown.

$^4\text{He}$  were grown at molar volume of  $17.7$  and  $20.3$  cm<sup>3</sup>. At both densities, anomalies similar to those in  $^3\text{He}$  were observed. Figure 8 shows the anomaly in an hcp  $^4\text{He}$  crystal grown at  $17.7$  cm<sup>3</sup>/mole. The anomaly is similar to those previously observed<sup>6,7</sup> in "well-annealed" hcp  $^4\text{He}$  crystals at  $17.4$  and  $20.32$  cm<sup>3</sup>/mole.

The crystals grown at  $20.3$  cm<sup>3</sup>/mole had such large attenuation at low temperatures that measurements were not possible below 1 K. As a result, no

TABLE I. Dislocation parameters.

Crystal	Isotope	Phase	Molar volume (cm <sup>3</sup> )	$\nu$ (m/sec)	$l_c$ (cm)	$L$ (cm)	$RA$ (cm <sup>-2</sup> )	$g$ ( $B = gT^3$ ) (cgs units)	$RAL^2$
2	$^3\text{He}$	hcp	18.6	830	$4.24 \times 10^{-3}$	$5.94 \times 10^{-4}$	$4.28 \times 10^3$	$1.00 \times 10^{-7}$	0.0015
3	$^3\text{He}$	hcp	18.6	830	$4.24 \times 10^{-3}$	$1.02 \times 10^{-3}$	$1.70 \times 10^2$	$1.00 \times 10^{-7}$	0.0018
5	$^3\text{He}$	hcp	18.6	870	$4.24 \times 10^{-3}$	$6.37 \times 10^{-3}$	$1.84 \times 10^3$	$1.41 \times 10^{-7}$	0.075
7	$^3\text{He}$	hcp	17.8	1008	$5.62 \times 10^{-3}$	$7.30 \times 10^{-4}$	$4.30 \times 10^3$	$5.73 \times 10^{-8}$	0.0023
36	$^3\text{He}$	bcc	20.1	792	$3.58 \times 10^{-3}$	$9.66 \times 10^{-4}$	$2.62 \times 10^3$	$2.76 \times 10^{-7}$	0.0024
43	$^3\text{He}$	bcc	20.1	745	$3.58 \times 10^{-3}$	$9.38 \times 10^{-4}$	$1.96 \times 10^3$	$2.70 \times 10^{-7}$	0.0017
1	$^4\text{He}$	hcp	17.7	723	$2.92 \times 10^{-3}$	$3.80 \times 10^{-4}$	$2.69 \times 10^3$	$2.24 \times 10^{-7}$	0.0004



velocity anomaly was observed and no dislocation parameters could be determined although the very large attenuation was taken as an indication that the dislocation density  $RA$  was large.

#### D. Summary of results

Both hcp and high-density bcc  $^3\text{He}$  were observed to have anomalies similar to those found in hcp  $^4\text{He}$ . The dislocation parameters derived from fitting the velocity anomalies to the Granato-Lücke theory of dislocation-sound-wave interactions are listed in Table I.

#### V. DISCUSSION

The results reported here may be directly compared to previous work on hcp  $^4\text{He}$  (Refs. 5–7) and on bcc  $^3\text{He}$  at low densities.<sup>11,12</sup> In hcp  $^4\text{He}$ , both the magnitude of the adiabatic temperature dependence and the size of the anomaly are consistent with previous measurements. The absence during cooling of any anomaly in bcc  $^3\text{He}$  at 24.2  $\text{cm}^3/\text{mole}$  also agrees with previous observations as does the size of the adiabatic velocity change. The most significant result of the experiments reported here is the observation of an anomaly in hcp and high-density bcc  $^3\text{He}$  and its interpretation in terms of dislocations.

The extent to which the dislocation theory explains the observed anomaly may be judged from the quality of the velocity fits and from the comparison between the predicted and observed attenuation. One of the most stringent tests of the Granato-Lücke theory is its frequency dependence. The theory predicts that any negative-velocity anomaly must eventually become positive at sufficiently high frequency. Further increases in sound frequency result in a smaller but still positive anomaly. This prediction is due to the resonance nature of the vibrating-string model and is independent of the choice of loop-length distribution. The observed velocity anomaly always shows this frequency dependence, giving strong support to this dislocation explanation. The quantitative differences between the predicted and measured sound velocities at different frequencies may be due to the choice of an exponential loop-length distribution, as discussed by Iwasa *et al.*<sup>7</sup>

The attenuation predicted by the Granato-Lücke theory involves no additional adjustable parameters and therefore provides another test of the theory. The dislocation predictions agree qualitatively with

the measurements. That is, the relative size of the attenuation at different frequencies and the approximate temperatures of attenuation maxima are correctly predicted. In some crystals (e.g., Fig. 5) the magnitude of the predicted attenuation is nearly correct, while in others (e.g., Fig. 8) it is several times too small.

It was observed that adding 0.53%  $^4\text{He}$  to the  $^3\text{He}$  eliminated the anomaly. This supports the dislocation explanation of the anomaly, since impurities are expected to bind to dislocations and pin them.

The magnitude of the anomaly is reflected in the dislocation density  $RA$ . As can be seen from Table I, in hcp  $^3\text{He}$  this varies by a factor of about 25 from sample to sample, but the value of  $RA$  in the bcc  $^3\text{He}$  crystals varies only by about 30%. About five other crystals were grown from  $^3\text{He}$  containing small  $^4\text{He}$  concentrations (up to 430 ppm). These had similar anomalies, and they too had large variations of  $RA$  between hcp crystals, but only small variations between bcc crystals. Some of the variation in  $RA$  may be due to real differences in the dislocation density  $\Lambda$  but some must also be due to the orientation factor  $R$ . The observed range of sound velocities at a particular density (10% in hcp  $^3\text{He}$ , 15% in bcc  $^3\text{He}$ ) indicates that, in both phases, crystals were grown with a wide range of orientations. The orientation factor  $R$  varies between 0 and about 0.13 in hcp crystals. In bcc crystals, however, there is much less anisotropy in  $R$ . The large range of  $RA$  observed in hcp  $^3\text{He}$  and the much smaller range in bcc  $^3\text{He}$  thus agree qualitatively with the expected orientation dependence of  $R$ . In order to make quantitative comparisons, measurements in oriented crystals are needed.

Despite the variations in  $RA$  and the somewhat smaller variation in  $L$ , the values of  $B$  agree fairly well in crystals at the same density. The two damping mechanisms mentioned earlier, anharmonicity<sup>19</sup> and fluttering,<sup>20</sup> predict at low temperatures damping proportional to  $T^5$  and  $T^3$ , respectively. At sufficiently low temperatures, the fluttering mechanism should be dominant and, since the observed damping is proportional to  $T^3$  comparisons may be made to the predicted damping due to the fluttering mechanism. According to Ninomiya,<sup>20</sup> the low-temperature damping is

$$B_f \simeq \frac{14.4k_B}{\pi h^2 c^3} T^3 \quad (T \ll \Theta_D), \quad (12)$$

where  $k_B$  is Boltzmann's constant,  $h$  is Planck's constant, and  $c$  is an average sound velocity which

may be taken as the Debye velocity. For bcc  $^3\text{He}$  at  $20.1 \text{ cm}^3/\text{mole}$  ( $c \approx 310 \text{ m/sec}$ ), the fluttering value is  $B_f \approx 1.1 \times 10^{-7} T^3$  cgs units compared to the observed values of  $B \approx 2.7 \times 10^{-7} T^3$  cgs units. In hcp  $^3\text{He}$  at  $18.6 \text{ cm}^3/\text{mole}$ ,  $B_f \approx 4.3 \times 10^{-8} T^3$  cgs units, while the observed values are  $(1-1.4) \times 10^{-7} T^3$  cgs units. Considering the uncertainties in the theoretical value of  $B_f$  and in determining  $B$  from the data, the agreement is quite good. The observed decrease in  $B$  when the density was increased from  $18.6$  to  $17.8 \text{ cm}^3/\text{mole}$  is also in agreement with the fluttering prediction.

The dimensionless combination of dislocation parameters  $\Lambda L^2$  is characteristic of the dislocation network. For a perfect cubic network of dislocations,  $\Lambda L^2 = 3$ . However, any additional pinning of dislocations (e.g., by point defects) will reduce  $L$  so that  $\Lambda L^2 < 3$ . In addition, using a distribution of loop lengths changes the value of  $\Lambda L^2$ .

Values of the product  $R\Lambda L^2$  are listed in the last column of Table I. If an average value of  $R$  of 0.05 is chosen, then the values of  $\Lambda L^2$  range from about 0.01 to 1.5. Since the exponential distribution of loop lengths used is more appropriate to the case of pinning by random point defects than to network pinning, the result  $\Lambda L^2 < 3$  is not surprising.

In conclusion, the Granto-Lücke theory of dislocation resonance is able to qualitatively explain both the velocity and attenuation of longitudinal sound in bcc and hcp  $^3\text{He}$ . The observed sound anomaly and the dislocation parameters determined by fitting the theory to the anomaly are similar to those previously found in hcp  $^4\text{He}$ . The damping has the  $T^3$  temperature dependence typical of the fluttering mechanism and approximately the correct magnitude. Below 1 K, the dislocations become undamped and vibrate freely, resulting in a large anomaly. The smallness of the elastic constants of helium results in low resonant frequencies of the dislocation loops. These factors allowed the transition from a low-frequency negative-velocity anomaly to a high-frequency positive-velocity one to be observed in some crystals when the frequency was increased from 3 to 21 MHz.

#### ACKNOWLEDGMENTS

The authors would like to thank Dr. I. Iwasa for helpful discussions and A. O'Shea for help with the experiments. This work was supported in part by grants from the Natural Sciences and Engineering Research Council of Canada.

- \*Present address: Physics Department, Brown University, Providence, R. I. 02906.
- <sup>1</sup>R. A. Guyer, R. C. Richardson, and L. I. Zane, *Rev. Mod. Phys.* **43**, 532 (1971).
- <sup>2</sup>V. J. Minkiewicz, T. A. Kitchens, G. Shirane, and E. G. Osgood, *Phys. Rev. A* **8**, 1513 (1973).
- <sup>3</sup>B. M. Guenin and A. J. Dahm, *Phys. Rev. B* **23**, 1139 (1981).
- <sup>4</sup>D. J. Sanders, H. Kwun, A. Hikata, and C. Elbaum, *Phys. Rev. Lett.* **39**, 815 (1977).
- <sup>5</sup>R. Wanner, I. Iwasa, and S. Wales, *Solid State Commun.* **18**, 853 (1976).
- <sup>6</sup>I. D. Calder and J. P. Franck, *Phys. Rev. B* **15**, 5262 (1977).
- <sup>7</sup>I. Iwasa, K. Araki, and H. Suzuki, *J. Phys. Soc. Jpn.* **46**, 1119 (1979).
- <sup>8</sup>A. V. Granato and K. Lücke, *J. Appl. Phys.* **27**, 583 (1956).
- <sup>9</sup>M. A. Paalanen, D. J. Bishop, and H. W. Dail, *Phys. Rev. Lett.* **46**, 664 (1981).
- <sup>10</sup>V. L. Tsymbalenko, *Zh. Eksp. Teor. Fiz.* **74**, 1507

- (1978) [*Sov. Phys.—JETP* **47**, 787 (1978)].
- <sup>11</sup>R. Wanner, K. H. Mueller, and H. A. Fairbank, *J. Low Temp. Phys.* **13**, 153 (1973).
- <sup>12</sup>I. Iwasa and H. Suzuki (unpublished).
- <sup>13</sup>I. Iwasa and H. Suzuki, *J. Phys. Soc. Jpn.* **49**, 1722 (1980).
- <sup>14</sup>J. R. Beamish and J. P. Franck, *Phys. Rev. Lett.* **47**, 1736 (1981).
- <sup>15</sup>Crystals were analyzed at the Helium Resource Center, U.S. Bureau of Mines, Amarillo, Texas.
- <sup>16</sup>B. M. Abraham, Y. Eckstein, J. B. Ketterson, M. Kuchnir, and P. R. Roach, *Phys. Rev. A* **1**, 250 (1970).
- <sup>17</sup>J. Holder, *Rev. Sci. Instrum.* **41**, 1355 (1970).
- <sup>18</sup>F. Tsuruoka and Y. Hiki, *Phys. Rev. B* **20**, 2702 (1979).
- <sup>19</sup>A. D. Brailsford, *J. Appl. Phys.* **43**, 1380 (1972).
- <sup>20</sup>T. Ninomiya, *J. Phys. Soc. Jpn.* **36**, 399 (1974).
- <sup>21</sup>E. G. Henneke and R. E. Green, *Trans. AIME* **239**, 231 (1967).
- <sup>22</sup>R. E. Green and T. Hinton, *Trans. AIME* **236**, 435 (1966).